AUTHOR(S): KHOBRAGADE, P.S., HANSORA, D.P., NAIK, J.B., NJUGUNA, J. and MISHRA, S.

TITLE: Effect of multi-layered nanostructures on the physico-mechanical properties of ethylene vinyl acetate based hybrid nanocomposites.

YEAR: 2018

Effect of multi-layered nanostructures on the physico-mechanical properties of ethylene vinyl acetate based hybrid nanocomposites

Prashant S. Khobragade[1], D. P. Hansora[1], Jitendra B. Naik[1], James Njuguna[2], Satyendra Mishra[1]*

[1]University Institute of Chemical Technology, North Maharashtra University, Jalgaon-425001, Maharashtra, India

[2]School of Engineering, Robert Gordon University, Riverside East, Aberdeen, AB10 7GJ, United Kingdom

*Corresponding author's Email address: profsm@rediffmail.com (Satyendra Mishra)

Tel.: +91-257-2258420. Fax: +91-257-2258403

Abstract

Exfoliated graphene oxide (GO) and Mg-Al layered double hydroxides (LDHs) nanostructures (LDHs@GO) filled ethylene vinyl acetate (EVA) based hybrid nanocomposites were prepared by solution reflux technique followed by injection molding. The physico-mechanical (including morphological, thermal and mechanical) properties of LDHs@GO based layered nanostructures and EVA/LDHs@GO (0-1 wt. %) based hybrid nanocomposites were analyzed by field emission scanning electron microscopy, fourier transform infrared spectroscopy, wide and low angle X-ray diffraction spectroscopy, differential scanning calorimetry, thermogravimetric analysis and mechanical (tensile and elongation at break) testing. The morphological studies revealed that LDHs sheets were homogeneously inserted in between GO sheets, while LDHs@GO based layered nanostructures were found to be easily exfoliated in EVA/LDHs@GO hybrid nanocomposites up to 0.7 wt. % loading after which agglomeration occurred. The thermal stability of the hybrid nanocomposites was found to be improved at highest LDHs@GO loading of 0.7 wt. %. Mechanical properties (tensile strength and elongation at break) of the hybrid nanocomposites were observed to be enhanced by 70 and 80 % respectively at LDHs@GO loading of 0.7 wt. % and highest values of mechanical properties were obtained. Though, the morphological, thermal and mechanical properties of the composites were improved, the FTIR analysis did not reveal any chemical interaction between EVA and the LDHs@GO based layered nanostructures. From the overall results, it is obvious that a significant synergism was observed in terms of morphological, thermal and mechanical properties of EVA/LDHs@GO hybrid nanocomposites with optimum (less than 1 wt. %) loading of LDHs@GO based layered nanostructures.

Keywords : Layered nanostructures, Mechanism, Hybrid nanocomposites, Properties

1. Introduction

Currently, ethylene vinyl acetate (EVA) is rapidly emerging to substitute traditional polymeric material in technical fields, due to their unique characteristics, such as high softness, good mechanical and physical properties, easy processing as well as good resistance to chemicals. EVA is highly flexible due to its chemical structure and also possesses low-temperature toughness, high resistivity to rupture as well as ultra-violet radiation and delivers high cohesive strength, compatibility and excellent adhesion to a wide range of substrates. This elastomeric copolymer can be found applicable, depending on its vinyl acetate content and its characteristic. But EVA copolymers are thermally unstable and burn in a rapid way, which reduces their use of various applications [1]. To make them usable, different fillers are added [2]. However, improvement in the physico-mechanical (thermal, mechanical, physical) properties of EVA has become a significant topic [3], as high performance of materials, especially in field of insulating materials, hot melt adhesives, food packing [4], biomedical [5-6], photo voltaic [7], construction, lubricant, transport and electrical engineering applications.Traditionally unmodified and modified calcium carbonate [8-12], fly ash, carbon nanotubes (CNTs) [13], multi walled CNTs [14-16], carbon black, nanoclays [17,18], alumina clay [19], ZnO [20], Fe_3O_4 [21] and wollastonite [22] nanofillers are used to improve the physico-mechanical properties. Additionally, fillers are uniformly distributed or exfoliated with polymer matrix to form intermolecular interaction with polymer chains and to increase the properties of polymer nanocomposites. Nevertheless, high loading (3-4 wt. %) of inorganic nanofillers is needed to meet the requirement of improved physico-mechanical properties of polymer matrix. However, high content of inorganic nanomaterials may increase the cost. Researchers have already been using different fillers in various polymer matrices and reduced the production cost with enhancement of the multifunctional properties [23-25] and productivity [26-

30]. Addition of different hybrid nanostructures is another way to enhance physico-mechanical properties of EVA matrix. Moreover, the use of hybrid nanostructures can improve the same property by adding the less quantity (<1 wt. %) as compared to different nanomaterials [31].

In this work, a small content of LDHs@GO based layered nanostructures was employed to improve the physico-mechanical properties of EVA based hybrid nanocomposites. The aim of this work is to study the comparison of morphological, thermal and mechanical behavior for LDHs@GO filled EVA nanocomposites with different wt. % loading of layered nanostructures. The thermal stability and crystallization behavior of the nanocomposites were investigated by thermogravimetric analysis (TGA) and differential scanning calorimeter (DSC) analysis, respectively. And the intercalation and exfoliation of layered hybrid nanostructures in a polymer matrix were analyzed by field emission scanning electron microscope (FE-SEM) and X-ray diffractometer (XRD). The mechanical properties of the nanocomposites were measured using universal tensile testing machine (UTM).

2. Experimental

2.1 Materials

For the preparation of EVA hybrid nanocomposites, EVA-1815 thermoplastic copolymer with 15 % vinyl acetate was procured from Hanwha Chemicals, Korea and LDHs@GO multi layered nano structures was synthesized with Mg-Al–LDHs and GO by bath ultrasonication technique. Magnesium nitrate ($Mg(NO_3)_2 \cdot 6H_2O$), aluminium nitrate ($Al(NO_3)_3.9H_2O$) and graphite fine powder, hydrogen peroxide (H_2O_2), sulfuric acid (H_2SO_4), hydrochloric acid (HCl) and sodium nitrate ($NaNO_3$), potassium permanganate ($KMnO_4$) was used as a precursor for the synthesis of both Mg-Al LDHs and GO. All the precursors, anhydrous sodium carbonate, sodium hydroxide and sodium dodecyl sulfate (SDS) were also purchased from Rankem, India, Loba Chem, India, Merck,

India, consisting 98 % purity and Sigma Aldrich, India. Solvent (toluene) was procured from Merck, India. All the chemicals were of analytical reagent grade and were used without any further purification. Double distilled water was used throughout the experiments.

2.2 Synthesis of LDHs@GO based hybrid nanostructures

The LDHs@GO (1:1) based hybrid layered nanostructures were synthesized by using GO and SDS modified Mg-Al LDHs by bath ultrasonication technique [32]. For the preparation of layered hybrid nanostructures, 50 mL aqueous GO and equal amount of aqueous LDHs were taken in the weight ratio of 1:1 (LDHs@GO). The resulting dispersion of GO was sonicated for 15 min, while LDHs solution was added drop wise to the GO solution under bath sonication. The mixture was sonicated for 30 min more in order to form a colloidal dispersion. Lastly, the beaker containing LDHs@GO dispersion was placed for 48 h for settling. Finally, the resulting product was vacuum dried at 120 °C to remove any remaining traces of water.

2.3 Preparation of EVA/LDHs@GO hybrid nanocomposites

EVA/LDHs@GO based hybrid nanocomposites with 0.3, 0.5, 0.7, 0.9 and 1 wt. % loading of LDHs@GO based layered hybrid nanostructures were prepared by solution reflux technique [33]. The desired amount of EVA was dissolved in toluene and LDHs@GO based layered hybrid nanostructures were then added to the EVA solution. The temperature was increased up to the 140 °C under constant stirring after addition of LDHs@GO and refluxed for 20 h at 140 °C with vigorous stirring for exfoliation and increase in the rate of mixing of hybrid layered materials into the EVA matrix. Finally, the composite solution was cast and dried at room temperature for 5 days and then in a vacuum oven for 24 h at 75°C.

The mixed material of composites was then fed into an injection molding machine at 30 ^{o}C by keeping the temperatures at 90, 120 and 130 ^{o}C of the feed, compression and metering zones,

respectively. The molding process cycle was kept for the duration of 60 Sec. to prepare dumbbell shape specimens.

2.4 Characterizations

Morphology of GO, LDH sheets and LDHs@GO layered nanostructures and LDHs@GO filled EVA hybrid nanocomposites were determined by using FE-SEM (S-4800 Hitachi High. Tech, Tokyo, Japan) operated at an accelerating voltage of 30 kV. The size of nanostructures and hybrid nanocomposites was also measured directly by FE-SEM and TEM.

The FTIR transmission spectra of LDHs@GO layered nanostructures and LDHs@GO filled EVA hybrid nanocomposites were recorded on spectrophotometer (FTIR-8000, Shimadzu, Tokyo, Japan) at room temperature keeping 25 scans per sample. The resolution of the measurements was kept at 4 cm^{-1} and spectra were recorded within the wave number range from 400 to 4000 cm^{-1}.

To understand the effect on crystallinity of the LDHs@GO and their hybrid nanocompsites with EVA, the wide angle XRD patterns were recorded. The small angle XRD pattern was also recorded to measure the exfoliation and intercalation of hybrid nanostructures in the matrix by using X-ray diffractometer (XRD, Bruker D8 Advance, Germany) in the range of 0-60° and 5-15°.

Thermal behaviors and thermal degradation of LDHs@GO layered nanostructures, EVA and EVA/LDHs@GO hybrid nanocomposites were determined by using DSC-60 (Shimadzu, Tokyo, Japan) and TGA-50 (Shimadzu, Tokyo, Japan). Indium was employed for temperature calibration and nitrogen gas with a flux of ca. 50 mL/min was used to prevent oxidative degradation of samples. DSC and TGA thermograms were recorded within the range of -20 to 120 °C and 30 to 600 ºC respectively at a heating rate of 10 °C/min. The inflection point of the slope of the heat capacity plot was taken as the glass transition temperature (T_g). The mechanical properties like tensile strength (TS) and elongation at break (EB) were measured as per ASTM-D 412 standards

using testing machine (UTM 2302, High Tech Instruments, Mumbai, India) with a crosshead speed of 50 mm/min. The mechanical testing was performed five times and then analyzed. The mean value of five samples was taken and plots were generated.

3. Results and discussion

3.1 Morphology of LDHs@GO layered nano structures

The FE-SEM micrographs of GO, LDH sheets and LDHs@GO layered nanostructures are shown in Fig. 1 (a-c) and TEM micrographs are as inset in Fig. 1 (a-c), which indicated that the GO exhibit the highly exfoliated layers with an average thickness of 50 nm and up to the certain μm in length (Fig. 1a) [34-37]. The LDH sheets are consisted of regular and thin hexagonal single platelets and highly exfoliated structures with an average thickness of 25 nm and length up to the 250 nm, which is indication of nanoscale size [38, 39]. The morphology of the LDHs@GO layered nanostructures are shown in FE-SEM and TEM micrographs (Fig. 1c). The corresponding images show that LDH sheets have been uniformly inserted into GO inter layers and considerably amplifies the distances between adjacent GO sheets and make them layered hybrid nanostructures [32].

3.2 FTIR analysis of EVA/LDHs@GO hybrid nanocomposites

FTIR analysis was used to detect the structural and chemical changes in EVA/LDHs@GO hybrid nanocomposites. The FTIR spectra of nano composites are shown in Fig. 2. From Fig. 2 all the spectra show strong absorbance peaks around 2850 and 2920 cm^{-1}, associated with the C-H asymmetric stretching of the polymer. The peak representing the vibration of the –C=O ester of the carbonyl group appears at 1650 to 1750 cm^{-1} in pure EVA (Fig. 2a). The spectra of EVA/LDHs@GO hybrid nanocomposites from 0-1 wt. % loading of layered LDHs@GO nanostructures shows a wide and intense peaks from 3000 to 3741 cm^{-1}, which are attributed to the

O-H band stretch (hydrogen bonding) of the GO and LDH crystal structure. The peaks at 2917 and 2849 cm^{-1}ascribed to the asymmetric and symmetric vibrations, respectively, of aliphatic groups (CH_2). The band at around 1237 cm^{-1} is attributed to the asymmetric vibration of C-O-C stretching. The bands at around 1019 and 720 cm^{-1} are ascribed to the metal oxygen in plane stretching and deformation. The FTIR spectral analyses of EVA and its EVA/LDHs@GO hybrid nanocomposites show that the addition of LDHs@GO layered nanostructures into the EVA matrix enhances the width and intensity of the peak at 3000 - 3741 cm^{-1} and no chemical changes was observed in the EVA matrix after incorporation of LDHs@GO layered nanostructures, which suggest that the only hybrid nano structures might be exfoliated and intercalated properly into the EVA matrix [40-42]. Absence of any chemical reaction between EVA and LDHs@GO was supported by the FE-SEM and DSC results of hybrid nano composites.

3.3 Structural and morphological properties of EVA/LDHs@GO based hybrid nanocomposites

After introducing the LDHs@GO layered nanostructures with various loadings from 0-1 wt. % into EVA matrix, the obtained EVA/LDHs@GO hybrid nanocomposites were analyzed using XRD to study crystalline behavior. Fig. 3 and Fig. 4 show the wide and small angle XRD pattern of EVA/LDHs@GO hybrid nanocomposites with different loading of LDHs@GO layered nanostructures. In case of the neat EVA, sharp typical diffraction peaks are clearly observed at 2θ = 20.48º, 22.73º, 35.33º, 39.13º and 52.63º. For 0.3, 0.5 and 0.7 wt. % of LDHs@GO layered nanostructures loaded composites, the XRD peaks and their intensity are almost absent as compared to that of the neat EVA, this is directly vice versa with increasing the LDH loadings, the intensity of the reflection is gradually increased. These results clearly indicate that the LDHs@GO layered

nanostructures have been successfully exfoliated into the EVA matrix using the solution reflux method [43]; and the peaks at lower angles, corresponding to greater *d* spacing of GO sheets are due to insertion of the LDH layered structures in between GO sheets [44]. Fig. 4 shows the low angle XRD patterns in the range of $\theta \leq 5^{o}$ for EVA/LDHs@GO hybrid nanocomposites with different loading of LDHs@GO layered nanostructures. From the Fig. 4 (a), it can be seen that the diffraction peak of exfoliated GO at $2\theta=10.11^{o}$attributed to the (002) plane at basal spacing 8.73Å, and peak intensity of modified LDH sheets are appearing at $2\theta=11.6^{o}$ to the (003) planes. EVA/LDHs@GO hybrid nanocomposites indicate that LDHs@GO layered nanostructures have been properly exfoliated. From wide angle XRD patterns, when the LDHs@GO layered nanostructures loadings further increase to 0.9 and 1wt. %, the EVA/LDHs@GO hybrid nanocomposites show intercalated or partially aggregated structures because of the relatively weak diffraction peaks layers marked by the asterisks (*) appeared (Fig. 3 e-f). These results show that the solution reflux technique favors the exfoliation of LDHs@GO layered nanostructures [45] without showing any diffraction peaks from ordered LDHs@GO hybrid nanostructured platelets. These results denote that LDHs@GO layered nanostructures are exfoliated into the EVA matrix up to the 0.7 wt. %. However, XRD results cannot be the absolute evidence for the exfoliation nanolayers, because at lower concentrations of layered nanofiller, the diffraction patterns may not be largely affected. Therefore FE-SEM observation has to be accompanied to resolve this issue [46]. In order to better understand the morphology of EVA/LDHs@GO hybrid nanocomposites, one must also have information from FE-SEM micrographs that can provide direct imaging of the morphology. XRD investigations can only definitively detect periodic packings of layers at the nanoscale, whereas FE-SEM micrographs permit the imaging of the actual LDHs@GO layered nanostructures layers and their exfoliation and also agglomerates over the micrometer and

nanometer length scales; thus, one can fully describe the morphology of the nanocomposites system [47]. In the FE-SEM micrographs of EVA/LDHs@GO hybrid nanocomposites, the neat EVA and its fractured cryogenically nanocomposite films are seen in Fig.5. For the EVA/LDHs@GO hybrid nanocomposites with low contents up to 0.7 wt. % of LDHs@GO layered nanostructures were detected with exfoliated nature in the EVA matrix (Fig.5 (d). On the other hand, in the EVA/LDHs@GO hybrid nanocomposites with high contents above 0.7 wt. % of LDHs@GO layered nanostructures, partial aggregates or intercalated platelets are observed (Fig.5 (e-f)), although they did not exhibit any ordered structural feature, which was confirmed by XRD patterns as shown in Fig.3. The presence of aggregated LDHs@GO layered nanostructures is probably due to the partial restacking of disordered LDHs@GO platelets in the EVA nanocomposites with high contents. When the amount of LDHs@GO layered nanostructures reaches a critical content, the distance among LDHs@GO layered nano platelets is so small that they can be stacked together easily due to van der Waal force of attraction. From these results, it is conjectured that the LDHs@GO layered nanostructures give better exfoliation at less than 1 wt. % loading [47, 48]. It is expected that the excellent exfoliation of LDHs@GO layered nanostructures contributes to significant improvement in thermal stability and mechanical properties of EVA/LDHs@GO hybrid nanocomposites.

3.4 Thermal properties

3.4.1 DSC analysis

Fig. 6 shows DSC curves of pristine EVA and the EVA/LDHs@GO hybrid nanocomposites. The glass transition temperature (T_g) and the melting transition temperature (T_m) increase with increase in wt. % loading of the LDHs@GO layered nanostructures up to the certain loading level of 0.7 wt. %. T_g and T_m of EVA/LDHs@GO hybrid nanocomposites with 0.3, 0.5 and 0.7 wt. % LDHs@GO

layered nanostructures are 50, 51, 62 and 87, 87, 91 °C, respectively, largely higher than that of pristine EVA (48 and 83 °C) and slightly decrease for 0.9 and 1 wt. % loading (64, 89 and 40, 86 °C) in agreement with the value in EVA/LDHs@GO hybrid nanocomposites. The LDHs@GO layered nanostructures are exfoliated in EVA matrix taking strong entanglement between EVA macromolecules at certain loading (0.7 wt. %). And further loading hinders the reinforcing interaction between macromolecular chains in EVA/LDHs@GO hybrid nanocomposites that results a decrease in glass transition and melting temperature of the EVA due to the filler-filler aggregation (Table 1).

3.4.2 Thermogravimetric analysis

It can be seen from Fig. 7 that all EVA/LDHs@GO hybrid nanocomposites show enhanced thermal stabilities as compared with pure EVA matrix. The thermal degradation process of pure EVA resin occurs in two steps. The first degradation steps ($d_{on}1$) are in the range of 275-310 °C which can be assigned to the evolution of acetic acid, whereas the second degradation steps ($d_{on}2$) are in the range of 395-440 °C which is due to the degradation of ethylene based chains present in EVA [51]. There is about 25 % weight loss in the range of 275-310 °C for the EVA/LDHs@GO hybrid nanocomposites, which can be attributed to the decomposition of LDHs@GO layered nanostructures and the thermo-oxidative degradation of EVA. It can be seen from Table 1 that the first thermal degradation temperatures ($d_{on}1$) of EVA/LDHs@GO hybrid nanocomposites are 280, 285, 310, 255 and 230 °C for 0.3, 0.5, 0.7, 0.9 and 1wt. %, respectively. At the same time, the second thermal degradation temperatures ($d_{on}2$) of the EVA/LDHs@GO hybrid nanocomposites are 400, 405, 440, 405 and 400 °C for 0.3, 0.5, 0.7, 0.9 and 1 wt. % loadings, respectively. These data indicate that the thermal degradation temperatures increase with increasing the wt. % loadings of

LDHs@GO layered nanostructures up to the 0.7 wt. % loading and then decreases. This is probably because the more loading of LDHs@GO layered nanostructures, layers favor the obstruct effect and formation of char in the polymer, which increases the thermal stability of the nanocomposites. From the previous study [45], it has been found that the thermal degradation temperatures of exfoliated samples via solution reflux technique are higher than those of the corresponding exfoliated samples via other technique. This is probably because the more LDHs@GO layered nanostructures prepared by the solution reflux technique can homogeneously exfoliate in the EVA matrix [45]. By considering the thermal improvement, 0.7 wt. % loading of the LDHs@GO layered nanostructures in the EVA was found highly dispersed and reported as the optimum loading. The pristine EVA resulted in the reduction of 98 % weight loss (W_L) (Fig. 7). If the LDHs@GO layered nanostructures loading are too high (above certain loading 0.7 wt. %) the thermal stability of the EVA/LDHs@GO hybrid nanocomposites is lowered and so it is not appropriate for perfect application [48]. It is believed that the thermal stability of EVA/LDHs@GO hybrid nanocomposites (with 0.3 to 0.7 wt. % loadings) was obviously enhanced during this stage. The last stage is apparently relevant to the thermal cracking of the carbonaceous conjugated polymer chains (0.9 and 1wt. %) [49].

3.5 Mechanical properties

Tensile strength (TS) and elongation at break (EB) of EVA/LDHs@GO hybrid nanocomposites at various wt. % loadings of LDHs@GO layered nanostructures are shown in Fig. 8. The TS of EVA/LDHs@GO hybrid nanocomposites was also shown in increasing trend up to 0.7 wt. % loading. This was due to proper exfoliation as well as uniform dispersion of nanostructures in the matrix, which results in intermolecular interaction with the matrix, and that enhances the elongation with an increase in tensile strength. (Fig.5 (d)). However, the TS was observed highest in

EVA/LDHs@GO hybrid nanocomposites with 0.7 wt. % loading. This indicated that better reinforcing interaction and exfoliation of LDHs@GO layered nanostructures was improved at very lower loading as compared to single nanomaterials. In contrary, at higher loading (0.9 and 1wt. %), the TS of EVA/LDHs@GO hybrid nanocomposites decreased due to agglomeration and filler-filler interaction of the LDHs@GO layered nanostructures [Fig.5 (e-f)]. These results may lead to less interfacial interaction between LDHs@GO layered nanostructures and EVA matrix resulted in a reduction in TS of EVA/LDHs@GO hybrid nanocomposites at 0.9 and 1wt. % loading of LDHs@GO layered nanostructures.

It is also evident from Fig. 8 that the EB of EVA/LDHs@GO hybrid nanocomposites increased up to 0.5 wt. % loading, decreased for 0.7 wt. % loading and again increased for 0.9 and 1 wt. % loadings of LDHs@GO layered nanostructures. At the early stage, due to proper exfoliation of LDHs@GO layered nanostructures, the enhancement of elongation is the high resistance exerted by well exfoliated LDHs@GO layered nanostructures against the chain deformation and the stretching resistance of the oriented polymer backbones in the galleries. In addition, an improvement in the mechanical properties can also be accounted on the basis of static adhesion strength as well as interfacial stiffness caused by the efficient stress transfer at the interface and elastic deformation originating from the increased wt. % of LDHs@GO layered nanostructures [50].

4. Conclusion

A small amount of LDHs@GO layered nanostructures (0-1wt. %) was introduced to improve the physico-mechanical properties of EVA/LDHs@GO hybrid nanocomposites. It revealed that LDHs@GO layered nanostructures exhibited a synergistic effect on physico-mechanical properties including morphological, thermal and mechanical properties. When an amount of 0.7 wt. % of LDHs@GO layered nanostructures incorporated in EVA matrix, EVA/LDHs@GO hybrid

nanocomposites showed highest tensile strength (21 MPa) and d_{on} (310 °C) due to the greater reinforcing interaction and exfoliation of LDHs@GO. Further loading shows decrement in thermal stability and mechanical properties and this could be attributed to agglomeration and filler-filler interaction of LDHs@GO layered nanostructures due to the higher amount of filler. These properties of EVA/LDHs@GO nanocomposites are remarkably superior to those of pristine EVA or their conventional counterparts. Thus, preparation of EVA nanocomposites by reinforcement of LDHs@GO by solution reflux technique is an excellent method to obtain well hybrid nanocomposites. This opens the way to a wider industrial utilization of hybrid nanomaterials with good properties.

Acknowledgment

Prashant S. Khobragade is thankful and gratefully acknowledge to the University Grant Commission (UGC), New Delhi, Government of India for providing Rajiv Gandhi National Junior Research Fellowship [F1-17.1/2014-15/RGNF-2014-15-SC-MAH-58232/(SA-III/Website)]. Department of Science and Technology (DST-UKIERI), New Delhi, India [File No: DST/INT, UK/P-108/2014] is also acknowledged for financial support to carry out this research work.

References

[1] C. Feng, M. Liang, W. Chen, J. Huang, H. Liu, *J. Ana. App. Pyro.*, **111**, 266 (2015).

[2] R. ElHage, A. Viretto, R. Sonnier, L. Ferry, J. M. Lopez-Cuesta, *Polym. Deg. Stab.*, **108**, 56 (2014).

[3] S. Mishra, S. Sonawane, V. Chitodkar, *Polym. Plast. Tech. Eng.*, **44**, 463(2005).

[4] A. Sonia, K.P. Dasan, *J. Food Eng.*, 118 (1), 78 (2013).

[5] N. Pramanik, S. Mohapatra, P. Bhargava, P. Pramanik, *Mat. Sci. Eng. C.*, **29**, 228 (2009).

[6] M. Mousavi, S. Appendino, A. Battezzato, A. Bonanno, F. Chen Chen, M. Crepaldi, D. Demarchi, A. Favetto, F. Pescarmona, *Acta Astronaut.*, **97**,130 (2014).

[7] A. Jentsch, K. J. Eichhorn, B. Voit, *Polym. Testing.*, **44,242** (2015).

[8] S. Mishra, N.G.Shimpi, U.D. Patil, *J. Polym. Res.*, **14**, 449 (2007).

[9] S. Mishra, N.G.Shimpi, A.D. Mali, *Polym.for Adv. Tech.***23**, 236 (2012).

[10] S. Mishra, N. G. Shimpi, *J. App. Poly.Sci*.**98**, 2563(2005).

[11] S. Mishra, N. G. Shimpi, *J. App. Poly. Sci*.**64**, 744 (2005).

[12] S. Mishra, S. H. Sonawane, R.P. Singh, *J. Polym. Sci. Part B: Polym. Phy*.**43**, 107 (2005)

[13] G. Sui, W. H. Zhong, X. P. Yang, Y. H. Yu, S. H. Zhao, *Polym. Adv. Technol.*, **19**, 1543 (2008).

[14] N. Girun, F.R. Ahmadun, S. A. Rashid, *Fullerenes Nanotubes Carbon.*, **15**, 207 (2007).

[15] G. Beyer, *Fire Mater.*, **26**, 291 (2002).

[16] G. Beyer, *Wire Cable Technol. Int.*, **32**, 60 (2004).

[17] I. Ghasemi, M. Karrabi, M. Mohammadi, H. Azizi, *eXPRESS Polym. Lett*.,**4**, 62 (2010).

[18] S. Mishra, N.G. Shimpi, A. D. Mali, *Macromol. Res.*, **20**, 44 (2012).

[19] N. Mohamad, A. Muchtar, M. J. Ghazali, D. H. Mohd, C. H. Azhari, *Europ. J. Sci. Res.*, **24**,538(2008).

[20] M. Kalaee, S. Akhlaghi, S. Mazinani, A. Sharif, Y. C. Jarestani, M. Mortezaei, *J. Therm. Anal.Calor.*,**110**, 1407 (2012).

[21] A. Mohammadi, M. Barikani, M. Barmar, *J. Mater. Sci.*,**48**, 7493 (2013).

[22] A. Chatterjee, P. S. Khobragade, S. Mishra, *J. Appl. Polm. Sci.* 2015, DOI: 10.1002/APP.42811.

[23] Q.Wang, Y. Luo, C. Feng, Z.Yi, Q. Qiu, L. X. Kong, Z. Peng, *J. Nanomater.*, **5**, (2012), DOI:10.1155/2012/782986.

[24] N. G. Shimpi, J. Verma, S. Mishra, *Polym. Plast.Technol. Eng.*,**48**, 997 (2009).

[25] S. Mishra, S. S. Sonawane, N. G. Shimpi, *Polym. Plast. Technol. Eng*,**48**, 265 (2009).

[26] K. T. Paul, S. K. Pabi, K. K. Chakraborty, G. B. Nando,*Polym.Comp.*,**30**, 1647(2009).

[27] W. H. Zhang, X. D. Fan, W. Tian, W. W. Fan, *eXPRESS Polym. Polym. Lett.*, **6**,532 (2012).

[28] H. Zhang, C. Wang, Y. Zhang, *J. Appl. Polym. Sci.*, **10**, (2014). DOI: 10.1002/APP.41309.

[29] A. A. Abdul-Lateef, M. Al-Harthi, M. A. Atieh, *Arab. J. Sci. Eng.*, **35**, 49 (2010).

[30] N. M. Ahmed, D. E. ElNashar, *Mater. Desig.*, **44,** 1 (2013).

[31] P. S. Khobragade, J. B.Naik, A. Chatterjee, *Polym. Bull* ,DOI 10.1007/s00289-016-1812-2

[32] P. S. Khobragade, D. P. Hansora, J. B. Naik, J. Njuguna, S. Mishra, *Appl. Clay Sci.*, **132**, 668(2016).

[33] T. Kuila, S. Bose, C. E. Hong, M. E. Uddin, P. Khanra, N.H. Kim, J. H. Lee,*Carbon*, **49**, 1033(2011).

[34] L. Zhang,Y. He, S. Feng, L. Zhang, L. Zhang, Z. Jiao, Y. Zhan, Y. Wang, *Ceram. Int.*,,**42**, 6178 (2016).

[35] A. P. Pino, A. Datcu, E. György, *Ceram. Int.*, DOI.*org*/10.1016/j.ceramint.2016.01.122.

[36] R. Oraon, A. D. Adhikari, S. K. Tiwari, T. S. Sahu, G. C. Nayak, *Appl. Clay Sci.*,**118**, 231 (2015).

[37] T. Kavinkumar, S. Manivannan, *Ceram. Int.*, **42**, 1769 (2016).

[38] Q. Yan, Q. Liu, J. Wang, *Ceram. Int.*,**42**, 3007(2016).

[39] M. Chakraborty, S. Dasgupta, S. Sengupta, J. Chakraborty, S. Ghosh, J. Ghosh, M. K. Mitra, A. Mishra, T. K. Mandal, D. Basu, *Ceram. Int.*,**38**, 941 (2012).

[40] C. I. Idumaha, A. Hassana, *Synth. Met.*,**212,** 91(2016).

[41] B. Amaraj, K. R. Yoon, *J. App. Polym. Sci.*,**108**, 4090 (2008).

[42] L. Wang, L. Song, Y. Hu, K. K. Richard, *Ind. Eng. Chem. Res.*, **52**, 8062 (2013).

[43] S. K. Cheng, C. C. Wang, C. W. Chen, *Polym. Eng. Sci.*, **43**, 1221 (2003).

[44] Z. Matusinovic, M. Rogosic, J. Sipusic, *Polym. Degrad .Stab.*, **94**, 95 (2009).

[45] M. Zhang, P. Ding, L. Du, B. Qu, *Mater. Chem. Phy.*,**109**, 206 (2008).

[46] T. Kuila, S. K. Srivastava, A. K. Bhowmick, A. K. Saxena, *Compos. Sci. Technol*., **68**, 3234 (2008).

[47] J. E. An, G.W. Jeon, Y. G. Jeong, *Fiber. Polym.*,**13**, 507 (2012).

[48] Y. Gao, J. Wu, Q. Wang, C. A. Wilkie, D. O'Hare, *J. Mater. Chem. A*,**2**, 10996 (2014).

[49] N. H. Huang, J. Q. Wang, *eXPRESS Polym. Lett.*, **3, 595** (2009).

[50] D. Basu, A. Das, K.W. Stöckelhuber, U. Wagenknecht, G. Heinrich, *Prog. Polym. Sci.*, **39**, 594 (2004).

[51] S. Mishra, S. Balkrishnan, R. Chandra, *J. Appl. Polym. Sci.*,**70**,1829 (1998).

Captions for Figure

Fig. 1. FE-SEM and TEM micrographs of (a) GO (b) SDS-modified Mg-Al LDH (c) LDHs@GO layered nanostructures

Fig.2. FTIR spectra of (a) EVA and its hybrid nanocomposites containing (b) 0.3, (c) 0.5, (d) 0.7, (e) 0.9 and (f) 1 wt. % of LDHs@GO layered nanostructures

Fig. 3. Wide angle XRD spectra of (a) EVA and its hybrid nanocomposites containing (b) 0.3, (c) 0.5, (d) 0.7, (e) 0.9 and (f) 1 wt. % of LDHs@GO layered nanostructures

Fig. 4. Small angle XRD spectra of (a) EVA and its hybrid nanocomposites containing (b) 0.3, (c) 0.5, (d) 0.7, (e) 0.9 and (f) 1 wt. % of LDHs@GO layered nanostructures

Fig. 5. FE-SEMmicrographs of (a) EVA and its hybrid nanocomposites containing (b) 0.3, (c) 0.5, (d) 0.7, (e) 0.9 and (f) 1 wt. % of LDHs@GO layered nanostructures

Fig. 6. DSC of (a) EVA and its hybrid nanocomposites containing (b) 0.3, (c) 0.5, (d) 0.7, (e) 0.9 and (f) 1 wt. % of LDHs@GO layered nanostructures

Fig.7. TGA of (a) EVA and its hybrid nanocomposites containing (b) 0.3, (c) 0.5, (d) 0.7, (e) 0.9 and (f) 1 wt. % of LDHs@GO layered nanostructures

Fig.8. TS and EB of EVA and its hybrid nanocomposites containing 0.3, 0.5, 0.7, 0.9 and 1 wt. % of LDHs@GO layered nanostructures

Caption for Table

Table 1. DSC and TGA results of EVA/LDHs@GO hybrid nanocomposites

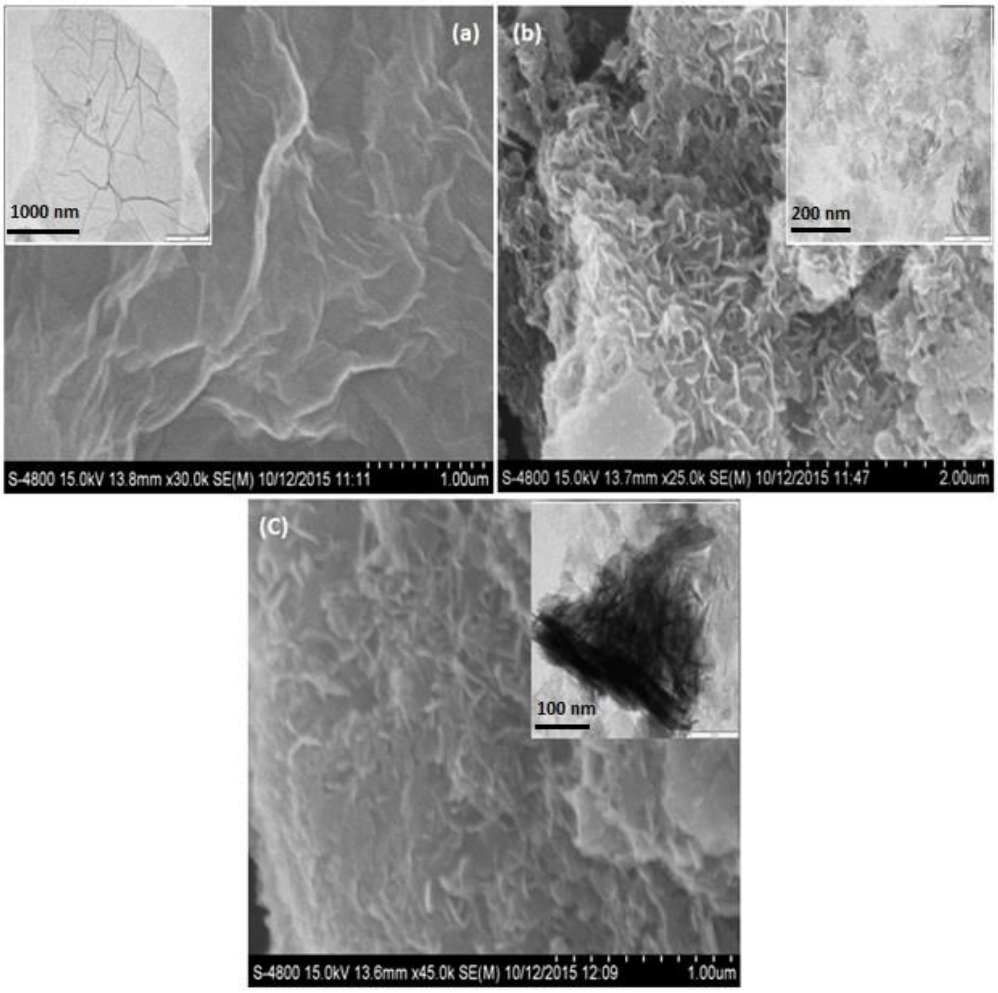
(a)
1000 nm
S-4800 15.0kV 13.8mm x30.0k SE(M) 10/12/2015 11:11 1.00um
(b)
200 nm
S-4800 15.0kV 13.7mm x25.0k SE(M) 10/12/2015 11:47 2.00um
(C)
100 nm
S-4800 15.0kV 13.6mm x45.0k SE(M) 10/12/2015 12:09 1.00um

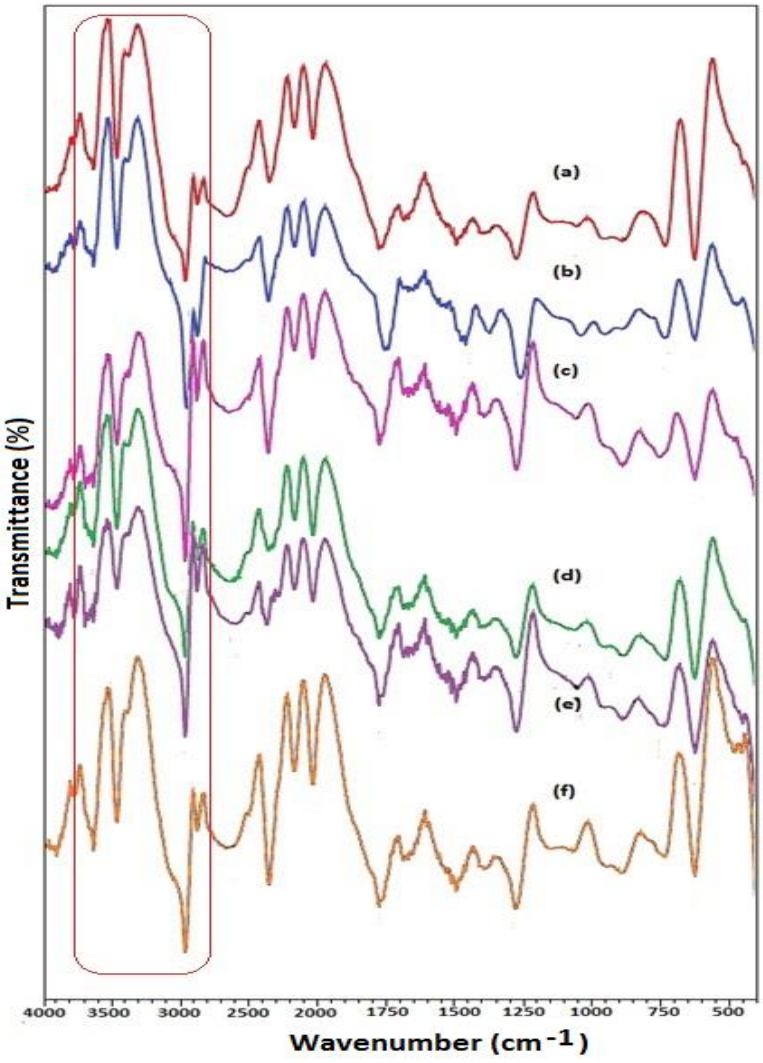
Transmittance (%)
(a)
(b)
(c)
(d)
(e)
(f)
4000
3500
3000
2500
2000
1750
1500
1250
1000
750
500
Wavenumber (cm-1)

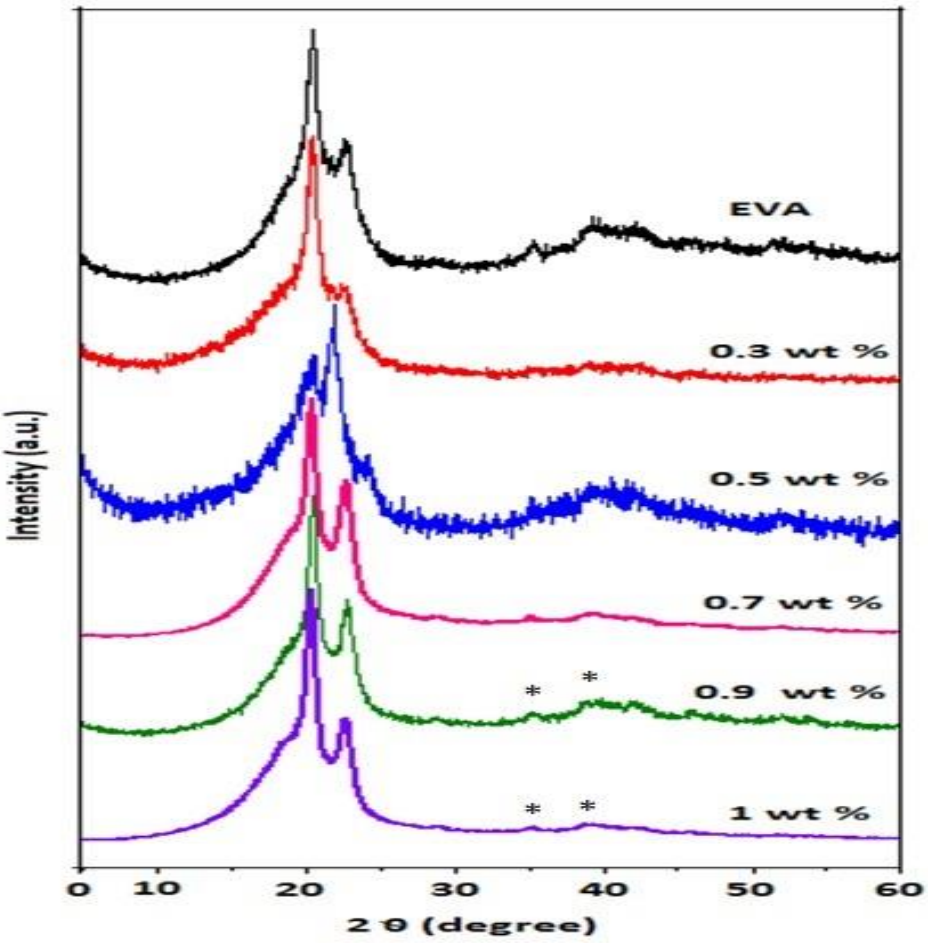
EVA
0.3 wt %
0.5 wt %
0.7 wt %
0.9 wt %
1 wt %
* *
* *
Intensity (a.u.)
0 10 20 30 40 50 60
2 θ (degree)

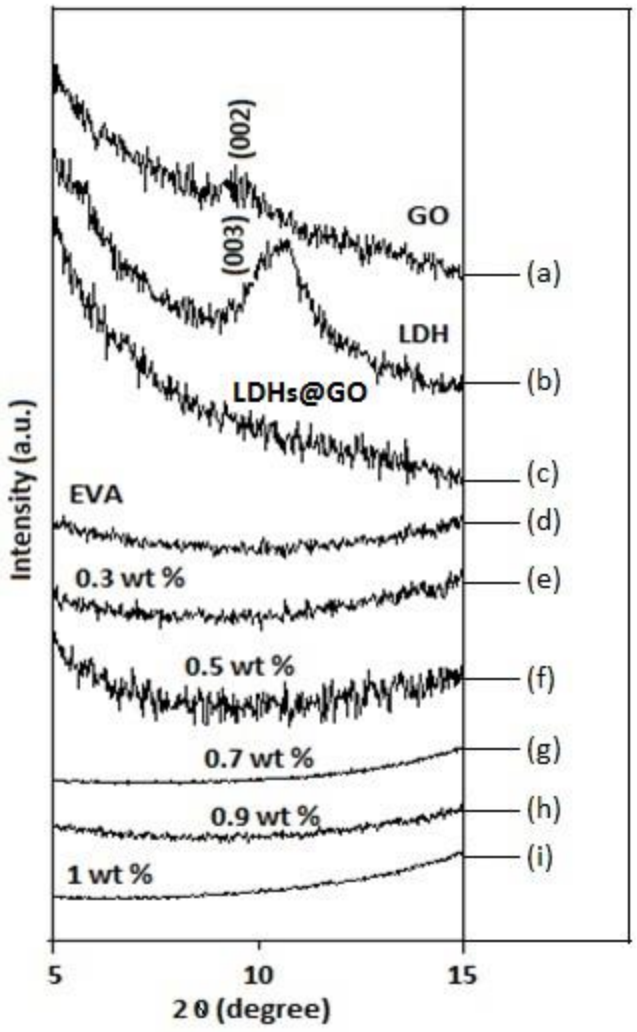
(002)
(003)
GO
LDH
LDHs@GO
EVA
0.3 wt %
0.5 wt %
0.7 wt %
0.9 wt %
1 wt %
(a)
(b)
(c)
(d)
(e)
(f)
(g)
(h)
(i)
Intensity (a.u.)
5
10
15
2 θ (degree)

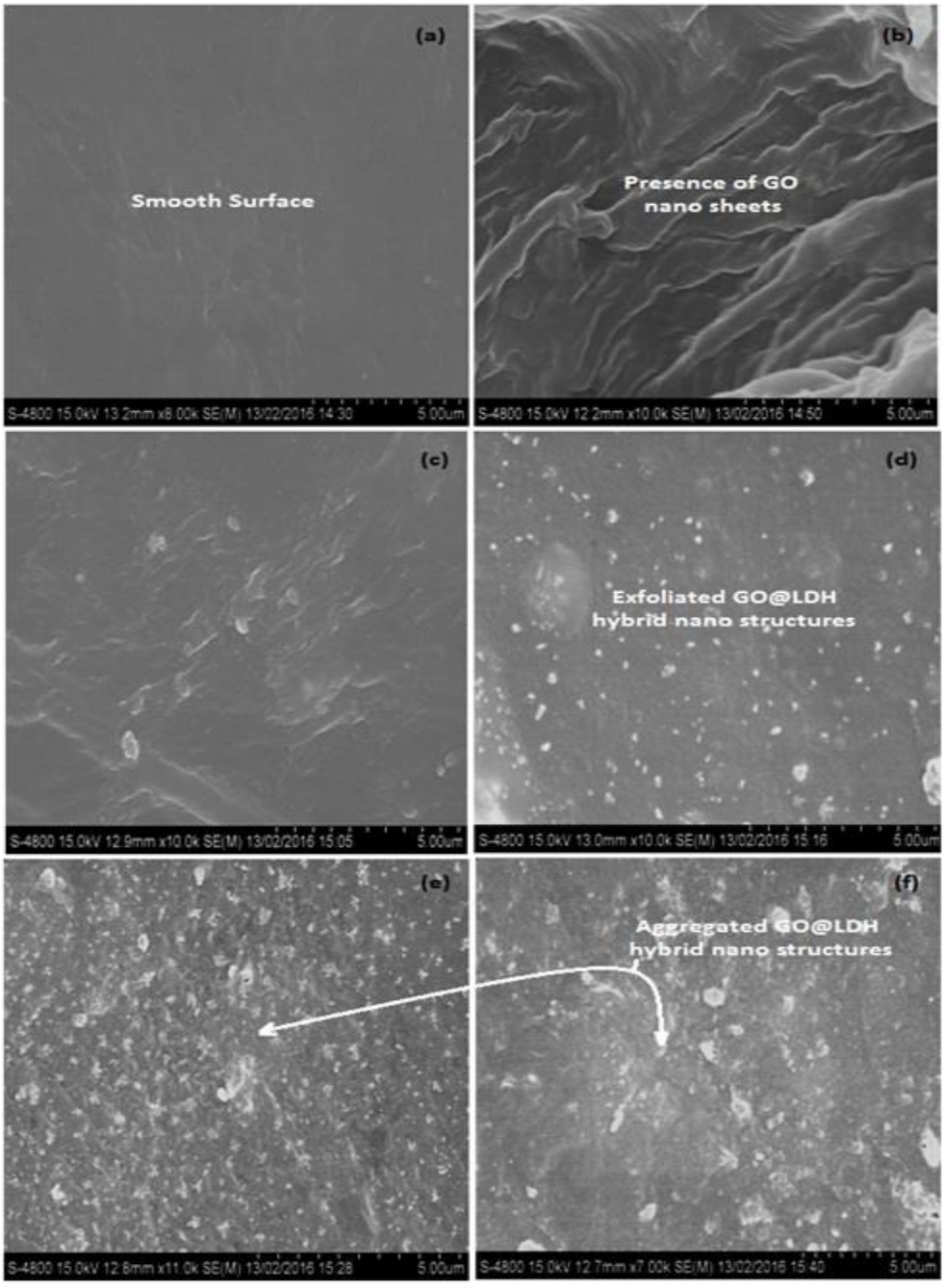
(a)
Smooth Surface
S-4800 15.0kV 13.2mm x8.00k SE(M) 13/02/2016 14:30 5.00um
(b)
Presence of GO
nano sheets
S-4800 15.0kV 12.2mm x10.0k SE(M) 13/02/2016 14:50 5.00um
(c)
S-4800 15.0kV 12.9mm x10.0k SE(M) 13/02/2016 15:05 5.00um
(d)
Exfoliated GO@LDH
hybrid nano structures
S-4800 15.0kV 13.0mm x10.0k SE(M) 13/02/2016 15:16 5.00um
(e)
S-4800 15.0kV 12.8mm x11.0k SE(M) 13/02/2016 15:28 5.00um
(f)
Aggregated GO@LDH
hybrid nano structures
S-4800 15.0kV 12.7mm x7.00k SE(M) 13/02/2016 15:40 5.00um

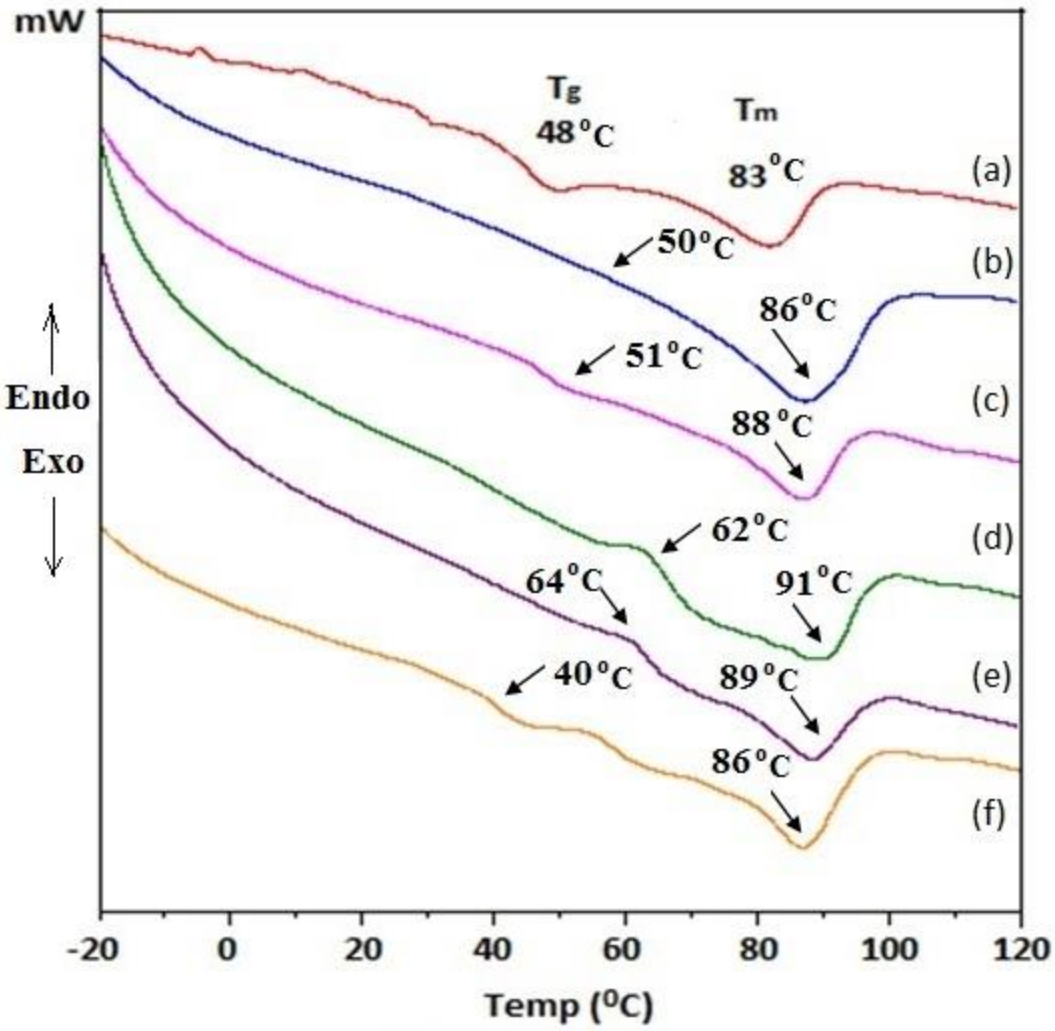
mW
Endo
Exo
Tg
48°C
Tm
83°C
(a)
50°C
(b)
86°C
51°C
(c)
88°C
62°C
(d)
64°C
91°C
40°C
89°C
(e)
86°C
(f)
-20
0
20
40
60
80
100
120
Temp (°C)

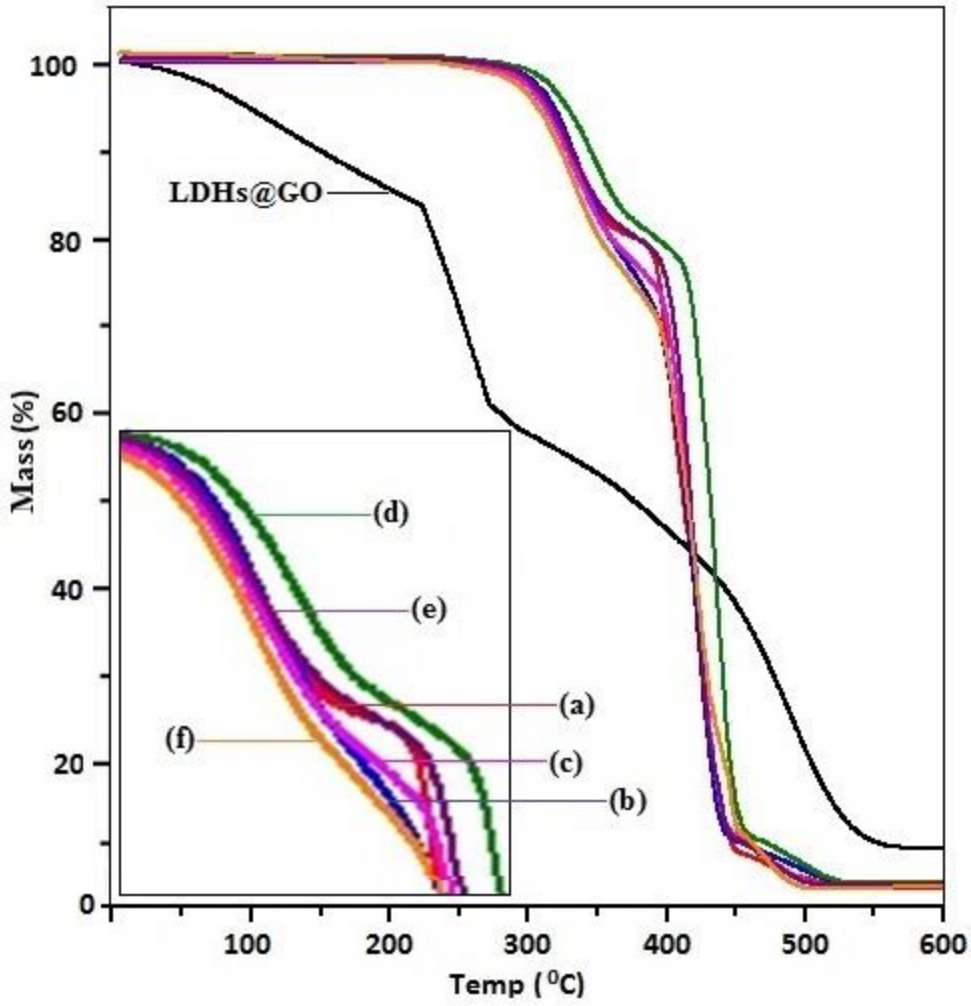
100
80
60
40
20
0
Mass (%)
100
200
300
400
500
600
Temp (^{0}C)
LDHs@GO
(d)
(e)
(a)
(f)
(c)
(b)

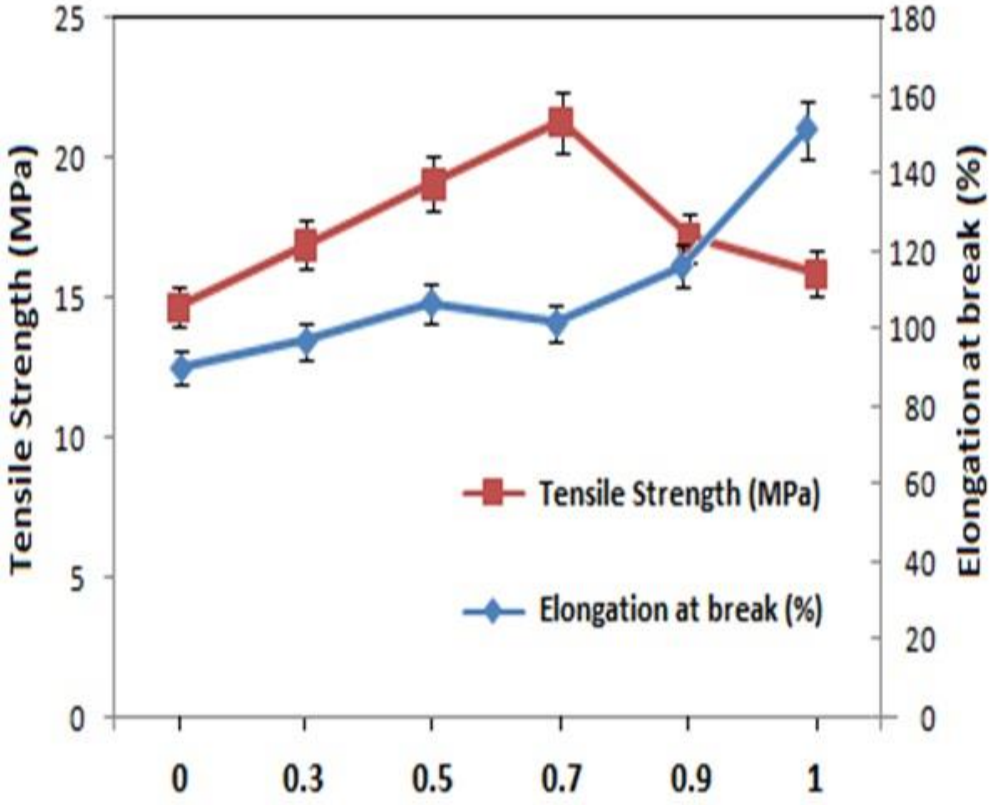
Tensile Strength (MPa)
Elongation at break (%)
25
20
15
10
5
0
180
160
140
120
100
80
60
40
20
0
0
0.3
0.5
0.7
0.9
1
Tensile Strength (MPa)
Elongation at break (%)

Table 1.

Wt. % of layered nanostructures in EVA nanocomposites	**T_g (°C)**	**T_m (°C)**	**$d_{on}1$ (°C)**	**$d_{on}2$ (°C)**	**D_{off} (°C)**	**W_L (%)**
0.0	48 (±1)	83 (±1)	275 (±5)	395 (±5)	485 (±5)	99.12 (±1)
0.3	50 (±1)	86 (±1)	280 (±5)	400 (±5)	475 (±5)	98.85 (±1)
0.5	51 (±1)	88 (±1)	285 (±5)	405 (±5)	480 (±5)	98.52 (±1)
0.7	62 (±1)	91 (±1)	310 (±5)	440 (±5)	480 (±5)	97.32 (±1)
0.9	64 (±1)	89 (±1)	255 (±5)	405 (±5)	460 (±5)	98.50 (±1)
1.0	40 (±1)	86 (±1)	230 (±5)	400 (±5)	460 (±5)	98.23 (±1)